Resiliency-Oriented Planning of Transmission Systems and Distributed Energy Resources

Hossein Ranjbar, Seyed Hamid Hosseini, *Member, IEEE,* and Hamidreza Zareipour, *Senior Member, IEEE*

***Abstract*—This paper presents a two-stage stochastic planning model for transmission systems and distributed energy resources (DERs) considering power system resiliency. The model takes into account both normal and emergency conditions as well as the duration of each condition. The proposed model is formulated as a mixed-integer linear program to minimize the total investment cost of transmission lines and DERs, expected values of generators' operation cost in normal and emergency situations, and load shedding cost in emergency condition. The emergency scenarios are considered as moderate, severe, and complete damage states, which have different recovery times for transmission assets. The Benders decomposition technique is utilized to solve the optimization problem. Numerical results are demonstrated based on the IEEE 118-bus test system.**

***Index Terms*—Distributed energy resources, extreme weather events, transmission expansion planning, resiliency.**

NOMENCLATURE

A. Sets and indices

l, L^+, L	Index and sets of candidate and existing lines
d, D	Index and set of candidate location of DERs
s, Ω	Index and set of scenarios in normal operating condition
$s', \Omega^{'}$	Index and set of damage scenarios in emergency operating condition
t, T	Index and set of representative days in normal operating condition
t', T'	Index and set of representative days in emergency operating condition
h, H	Index and set of operating time intervals
b, B	Index and set of buses
g, G	Index and set of generators
w, W	Index and set of wind farms
$s(l), r(l)$	Indices of sending and receiving buses of line l

B. Parameters and constants

c_l	Annualized investment cost of candidate line l
c^{dg}, P^{dg}	Annualized capital cost and size of each DER unit, respectively
$p_s, p_{s'}$	Probabilities of normal and damage scenarios s and s', respectively
$\tau_t^n, \tau_{t',s'}^e$	Duration of representative day t in normal operating condition and duration of emergency day t' for scenario s', respectively
c_g	Operation cost of generator g
c^{om}	Operation and maintenance cost of each DER unit
x_d^{max}	Maximum number of DER units which can be installed at location d
$\varkappa_b^{sh}$	Load shedding penalty factor at bus b
$\varkappa_w^{wc}$	Wind curtailment penalty factor of wind farm w
c_b^{sh}	Load shedding cost at bus b in emergency operating condition
ϱ, D^{max}	Maximum penetration level of DER units and the peak load, respectively
$PW_{w,h,t,s}^f$	Forecasted production of wind farm w, day t, time interval h, and scenario s
$PD_{b,h,t,s}$	Amount of load at bus b, day t, time interval h, and scenario s
PL_l^{max}	Maximum capacity of line l
B_l	Susceptance of transmission line l
M	Sufficiently large positive number
P_g^{Max}	Maximum generation capacity limit of generator g
$PW_{w,h,t',s}^f$	Forecasted production of wind farm w, emergency day t', time interval h, and scenario s
$PD_{b,h,t',s}$	Amount of load at bus b, emergency day t', time interval h, and scenario s
$\mu_{l,h,t',s'}$	Binary parameter that is 0 if line l during time interval h, day t', and damage scenario s' is in damage state or connected to a damaged substation; 1 otherwise.
$\phi_{g,h,t',s'}$	Binary parameter that is 0 if generator g during time interval h, day t', and damage scenario s' is connected to a damaged substation; 1 otherwise.
$\psi_{w,h,t',s'}$	Binary parameter that is 0 if wind farm w during time interval h, day t', and damage scenario s' is in damage state or connected to a damaged substation; 1 otherwise.

C. Variables and functions

x_l, x_d	Binary and integer variables associated with candidate line l and candidate DER unit at location d, respectively
$P_{g,h,t,s}^n$	Power generation of generator g, time interval h, day t, and scenario s

H. Ranjbar is with the Centre of Excellence in Power System Control and Management, Department of Electrical Engineering, Sharif University of Technology, Tehran, Iran and a visiting PhD student at the Department of Electrical and Computer Engineering, Schulich School of Engineering, University of Calgary, Calgary, Alberta, Canada (e-mail: h_ranjbar@ee.sharif.edu)

S. H. Hosseini is with Centre of Excellence in Power System Control and Management, Department of Electrical Engineering, Sharif University of Technology, Tehran, Iran (e-mail: hosseini@sharif.edu)

H. Zareipour is with the Department of Electrical and Computer Engineering, Schulich School of Engineering, University of Calgary, Calgary, Alberta, Canada (e-mail: h.zareipour@ucalgary.ca)

$PLS^{n}_{b,h,t,s}$	Load shedding at bus b, time interval h, day t, and scenario s
$PL^{n}_{l,h,t,s}$	Power flow of line l, time interval h, day t, and scenario s
$\theta^{n}_{b,h,t,s}$	Voltage angle of bus b, time interval h, day t, and scenario s
$PWC^{n}_{w,h,t,s}$	Curtailed wind power of wind farm w, time interval h, day t, and scenario s
$P^{e}_{g,h,t',s',s}$	Power generation of generator g, time interval h, emergency day t', damage scenario s', and scenario s
$PLS^{e}_{b,h,t',s',s}$	Load shedding at bus b, time interval h, emergency day t', damage scenario s', and scenario s
$PL^{e}_{l,h,t',s',s}$	Power flow of line l, time interval h, emergency day t', damage scenario s', and scenario s
$\theta^{e}_{b,h,t',s',s}$	Voltage angle of bus b, time interval h, emergency day t', damage scenario s', and scenario s
$PWC^{e}_{w,h,t',s',s}$	Curtailed wind power of wind farm w, time interval h, emergency day t', damage scenario s', and scenario s

I. Introduction

NATURAL hazards, such as hurricanes, earthquakes, floods, wildfires, and snowstorms, are of the main causes of major outages in power systems [1], [2]. For example, a study by the US department of energy shows that extreme weather events were responsible for 58% of component outages in power systems across the US between 2003 and 2012 [3]. Major natural hazards, which are categorized as high-impact low-probability (HILP) events, impact a large portion of power grids and have major economic and social consequences. Available data on superstorm Irene and hurricane Sandy, which hit the Northeast of the US in 2011 and 2012 affected 6.7 and 8.7 million customers, with estimated $10 and $20 billions of damages to the power system infrastructures, respectively [4].

It is likely that the frequency and severity of such events could go up in the future as a result of climate change and global warming [3], [5]. Nevertheless, conventional power system planning models only focus on high-probability low-impact events [6]. Examples of these events include equipment breakdowns, human errors, and external interferences, which are usually considered as N-1 or N-2 criteria in the planning of power systems [7]. Such plans usually do not consider the collapse of a large portion of power systems.

Resilience is an emerging concept in power system studies dealing with HILP events. Several definitions have been provided for resilience by power and energy organizations worldwide, such as the CIGRE [8], the U.K. Energy Research Centre [9], and the Federal Energy Regulatory Commission (FERC) [10]. The recent definition provided by FERC [10] defines resilience as "*The ability to withstand and reduce the magnitude and/or duration of disruptive events, which includes the capability to anticipate, absorb, adapt to, and/or rapidly recover from such an event*". According to this definition, the key stages of power system resilience can be outlined as 1) anticipating and preparing to make the power system as robust as possible before any HILP event; 2) responding in a timely and effective manner to preserve the system functionality during any extreme event; 3) recovering as quickly as possible to the level before the occurrence of any disruptive event, and 4) adapting the operation and structure of the power system to prevent or mitigate the impacts of similar events in the future [11].

Previous research articles have discussed the aforementioned stages of power system resilience against HILP natural hazards. Generally, the available research works can be divided into resiliency assessment, short-term studies, and long-term planning. Resiliency assessment works are mainly focused on presenting metrics and quantitative frameworks to evaluate the resilience of the power system to HILP events. For example, [12]–[14] present comprehensive discussions on different metrics and techniques for resiliency assessment against weather-oriented HILP events. Short-term studies focus on the preventive and corrective actions before, i.e., days or weeks, during, and after the events [15]. These works mainly utilize islanded microgrids to minimize and recover disconnected loads [16]–[19]. In [19], for instance, a new optimization model is proposed to divide distribution systems into multi-microgrids to maximize load restoration after a HILP event using coordinated topology reconfiguration.

Papers on long-term planning, which are also the focus of this paper, are related to power system planning for providing robustness and adaptability against major future events [14]. In [20], a two-stage stochastic formulation is proposed for transmission and generation expansion planning to increase the power system resiliency to earthquakes. The model considers different ranges of earthquake events and their associated damage states for each power system element. In [21], a risk-based approach is presented to minimize the vulnerability of transmission systems to natural hazards by defining economic and risk indices. The authors in [22] present a distributionally robust optimization-based planning model for the hardening and construction of transmission lines to enhance the system resilience against extreme weather events. In [23], a robust planning model is proposed for the hardening and expansion of transmission lines to improve power system resiliency; the model incorporates resiliency requirements by a set of constraints called the p-robustness constraints. Reference [24] develops a resiliency assessment framework to determine the weak points of the power system against Typhoon disasters. The model also provides a planning portfolio for the hardening and construction of new lines at weak points to enhance the system resiliency. The authors in [25] and [26] propose tri-level and quad-level models, respectively, for substation, transmission and generation, and transmission planning considering only extreme weather events.

In addition to the reviewed resiliency-oriented planning papers which have focused on only the hardening and expansion of transmission systems, other technologies like distributed energy resources (DERs) have been utilized to improve the power system resiliency. In [27], a planning model is proposed

to integrate distributed series reactors into transmission grids to enhance power system resiliency against HILP events. In [28], a robust optimization-based grid hardening and distributed generation allocation is proposed to enhance the resiliency of distribution systems. Reference [29] investigates the impact of microgrids sizing and siting in transmission systems to increase power system resiliency against hurricanes. In [30], a resiliency assessment framework is proposed to investigate the impact of DERs on power system resilience; the work quantifies the resilience of the power system for different scenarios of the presence of DERs in the system, i.e., ranging from 0% to 50%, without determining the site and size of DER units. The authors in [31] present a multi-objective model for sizing and siting of battery storage systems and photovoltaic resources to improve power system resilience in which the event-induced failures are characterized by the concept of capacity accessibility. Reference [32] presents a bi-level model to identify investment portfolios including substation hardening, line construction, and DER utilization for enhancing power system resilience. The first level of the model in [32] determines network enhancements and, in the second level, the response and restoration of the power system after occurring HILP hazards are simulated using sequential Mote-Carlo simulation.

Previous research works on transmission system resiliency planning (e.g., [20]–[22], [32]) were mainly focused on emergency condition related to HILP events without considering the impact of the proposed plan on the normal operating status of the system. Moreover, the previous works have considered fail versus operational states of components and their recovery times (e.g., [27], [29], [31]). Besides, many electric utilities (e.g., Commonwealth Edison in Chicago) are planning to install DERs in strategic places to reduce the negative impact of HILP events [29], [33]. However, despite the efforts made on utilizing DERs for enhancing power system resiliency (e.g. [30]–[32]), the potential of DER units in a joint DER/transmission plan for high-voltage power system resiliency against HILP has not been fully explored.

The main contribution of this paper is thus to present a joint transmission system and DER planning model for improving power system resiliency such that both the normal and emergency operating situations and the duration of each situation are considered. Moreover, the emergency condition is modeled by a set of damage scenarios based on three damage states, i.e., moderate damage, severe damage, and complete damage for transmission system components. This paper extends the efforts in [20], [22], [29], [31], and [32] by presenting a resiliency-based planning model that considers system conditions not only under emergency but also under normal operations. The inclusion of normal operating conditions in the process leads to a plan that improves system resiliency while reducing system operational costs in normal condition. The present paper also builds on previous resiliency-oriented literature [21], [27]–[29], [31], and [34] by expanding the operation states of the damaged system to include moderate damage, severe damage, and complete damage states of components and their associated recovery times. This consideration avoids the over-design of the system and saves unnecessary costs. Furthermore, unlike [35]–[37], which utilize DERs to improve the operation of power systems in the long-term in the normal operation condition, and building on works that have used DERs to improve distribution system resiliency (e.g., [28], [34]), we propose to integrate DERs in the transmission system planning process to enhance the system operation during not only the emergency events but also during the normal operation condition. The advantage of this consideration is avoiding over-design in the planning process and saving unnecessary costs. Moreover, the model in [32] is computationally intensive and challenging for large-scale networks due to the utilization of sequential Monte-Carlo simulation and a heuristic algorithm based on the genetic algorithm; however, we utilize Benders decomposition along with pre-determined damage scenarios which has better computational performance and can be applied to large-scale power systems.

The rest of this paper is organized as follows. Section II explains the general structure of the proposed model. The mathematical formulation of the proposed model and scenario determination procedure are also presented in this section. Section III describes the solution methodology based on the Benders decomposition method. Simulation results and discussions are provided in section IV, and finally, conclusions and future works are presented in section V.

II. Model Description and Assumptions

Fig. 1 illustrates the general structure of the proposed transmission and DER planning model. The first stage of the model determines new transmission lines and DER units by minimizing the total investment cost and expected operation and load shedding costs for both normal and emergency conditions. In the second stage, the operation subproblems are solved for each scenario of normal and emergency conditions. The objective of the normal subproblems is the operation costs of conventional generators and a penalty cost on wind power curtailment and load shedding. However, the emergency subproblems are trying to minimize the total load shedding costs based on load importance factors of each bus.

A. Assumptions

In this paper, in line with previous research works, we make a set of assumptions as follows.

1) The investment decisions of new transmission lines and DER units are optimized for a single target year [27].
2) The HILP event occurs only one time in the target year.
3) The N-1 reliability constraints related to failures of lines and power plants in normal operating condition are not considered in this paper [22], [24]–[27]. However, these constraints can be integrated into the proposed model using “Line Outage Distribution Factors” and “Power Transmission Distribution Factors” as in [38].
4) We assume that power plants will not be damaged by HILP events based on the fact that they are usually built with high structural reliability against extreme weather events like hurricanes [20], [39].

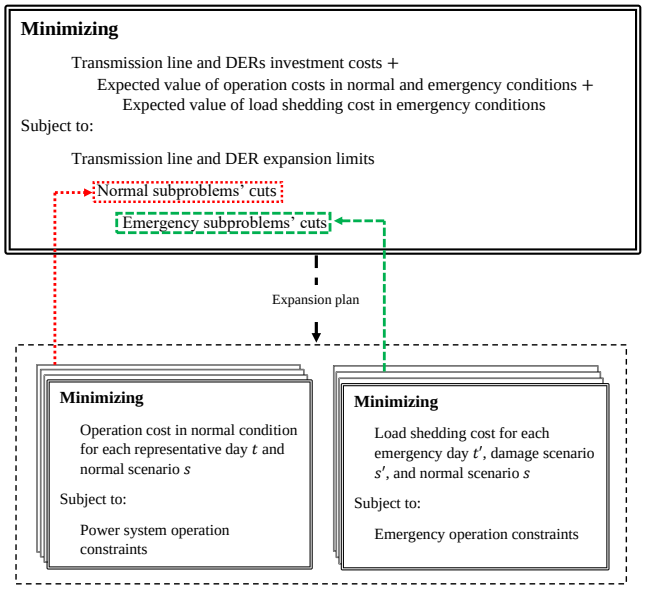

Fig. 1. Structure of the proposed model based on Benders decomposition.

5) The cascading outages of power system components associated with the induced HILP events are not considered in this paper [27], [32].
6) Wind farms, power plants, and transmission lines that are connected to a damaged substation will be disconnected for each damage scenario until it is recovered.
7) The DER units are considered as generic distributed generators with a linear operation and maintenance cost [35].
8) The uncertainties of future load and renewable energy production under normal condition are modeled by generating enough number of scenarios and then reducing them to a tractable number of scenarios using the fast-forward method (FFM) [35], [40]. The FFM first selects a subset of the original generated scenarios by minimizing the distance between the subset and remaining scenarios [40], [41]. Then, the probability of each non-selected scenario is added to its closest selected scenario according to their distance. For more detail see [40], [41].

B. Mathematical Formulation

The proposed two-stage resiliency-oriented stochastic transmission and DER planning model is as follows.

$$\min \sum_{l\in L^+} c_l x_l + \sum_{d\in D} c^{dg} P^{dg} x_d + \mathbb{E}[Q(x,\zeta)] \tag{1}$$

The first and second terms of (1) are the investment cost of new transmission lines and DER units, respectively. The third term is the expected value of operation and load shedding costs for both normal and emergency conditions. The mathematical representation of this term is as below:

$$\mathbb{E}[Q(x,\zeta)] = \sum_{s\in\Omega} p_s \left(Q^n(x,\zeta^s) + \sum_{s'\in\Omega'} p_{s'} Q^e(x,\zeta^s,\zeta^{s'}) \right) \tag{2}$$

where $\forall s \in \Omega$:

$$Q^n(x,\zeta^s) = \min \sum_{t\in T} \tau_t^n \sum_{h\in H} \Bigg(\sum_{g\in G} c_g P^n_{g,h,t,s} + \sum_{d\in D} c^{om} P^{dg} x_d + \sum_{b\in B} \varkappa_b^{sh} PLS^n_{b,h,t,s} + \sum_{w\in W} \varkappa_w^{wc} PWC^n_{w,h,t,s} \Bigg) \tag{3}$$

and $\forall s \in \Omega$ and $\forall s' \in \Omega'$:

$$Q^e(x,\zeta^s,\zeta^{s'}) = \min \sum_{t'\in T'} \tau^e_{t',s'} \sum_{h\in H} \sum_{b\in B} c_b^{sh} PLS^e_{b,h,t',s',s} \tag{4}$$

The first and second terms in (3) compute the operation costs of conventional generators and installed DER units and the third and fourth terms calculate load shedding and wind curtailment penalties under normal condition, respectively [27]. In this equation, $\varkappa_b^{sh}$ and $\varkappa_w^{wc}$ are load shedding and wind curtailment penalty factors which are considered large enough to avoid any curtailment in normal condition [42]. Similarly, (4) calculates the total cost of load shedding under emergency situation. Note that the load shedding cost parameter (c_b^{sh}) should be considered less than penalty factors in normal condition due to the high chance of load curtailment under emergency condition. However, it should be assumed in a way that the normal operation cost and emergency load shedding cost are comparable [27].

The constraints of the model include investment constraints, normal operational constraints, and emergency situation constraints [20], [27], [35]. Investment constraints are given as:

$$x_l \in \{0,1\}, x_d \le x_d^{max} \tag{5}$$

$$\sum_{d\in D} x_d P^{dg} \le \varrho D^{max} \tag{6}$$

where (5) represents the maximum number of new lines and DER units and (6) limits the integration level of DERs in the power system [35], [43].

The operational constraints for the normal condition for each scenario s, representative day t, and time interval h are as follows [35], [44].

$$\begin{aligned} &\sum_{g=b} P^n_{g,h,t,s} - \sum_{l|s(l)=b} PL^n_{l,h,t,s} + \sum_{l|r(l)=b} PL^n_{l,h,t,s} \\ &\quad + PLS^n_{b,h,t,s} - PD_{b,h,t,s} + \sum_{d=b} P^{dg} x_d \\ &\quad + \sum_{w=b} \left(PW^f_{w,h,t,s} - PWC^n_{w,h,t,s} \right) = 0 \ \forall b \in B \end{aligned} \tag{7}$$

$$-x_l PL_l^{max} \le PL^n_{l,h,t,s} \le x_l PL_l^{max};\ \forall l \in L^+ \tag{8}$$

$$-(1-x_l)M \leq PL^n_{l,h,t,s} - B_l(\theta^n_{s(l),h,t,s} - \theta^n_{r(l),h,t,s}) \leq (1-x_l)M;\ \forall l \in L^+ \quad (9)$$

$$-PL^{max}_l \leq PL^n_{l,h,t,s} \leq PL^{max}_l;\ \forall l \in L \quad (10)$$

$$PL^n_{l,h,t,s} - B_l(\theta^n_{s(l),h,t,s} - \theta^n_{r(l),h,t,s}) = 0;\ \forall l \in L \quad (11)$$

$$0 \leq P^n_{g,h,t,s} \leq P^{max}_g;\ \forall g \in G \quad (12)$$

$$0 \leq PLS^n_{b,h,t,s} \leq PD_{b,h,t,s};\ \forall b \in B \quad (13)$$

$$0 \leq PWC^n_{w,h,t,s} \leq PW^f_{w,h,t,s};\ \forall w \in W \quad (14)$$

In the above equations, (7) represents the supply-demand power balance constraint, (8)-(11) determine the power flows in the existing and new lines plus their flow limitations, and (12))-(14) limit the production of conventional generators, load shedding, and wind curtailment, respectively. The emergency condition constraints for each normal scenario s, emergency scenario s', emergency day t', and time interval h are as follows [20], [22], [23], [27].

$$\sum_{g=b} P^e_{g,h,t',s',s} - \sum_{l|s(l)=b} PL^e_{l,h,t',s',s} + \sum_{l|r(l)=b} PL^e_{l,h,t',s',s} + PLS^e_{b,h,t',s',s} - PD_{b,h,t',s} + \sum_{d=b} P^{dg} x_d + \sum_{w=b} \left(PW^f_{w,h,t',s} - PWC^e_{w,h,t',s',s}\right) = 0\ \forall b \in B \quad (15)$$

$$-(1-x_l)M \leq PL^e_{l,h,t',s',s} - B_l(\theta^e_{s(l),h,t',s',s} - \theta^e_{r(l),h,t',s',s}) \leq (1-x_l)M;\ \forall l \in L^+ \quad (16)$$

$$-x_l PL^{max}_l \leq PL^e_{l,h,t',s',s} \leq x_l PL^{max}_l;\ \forall l \in L^+ \quad (17)$$

$$-(1-\mu_{l,h,t',s'})M \leq PL^e_{l,h,t',s',s} - B_l(\theta^e_{s(l),h,t',s',s} - \theta^e_{r(l),h,t',s',s}) \leq (1-\mu_{l,h,t',s'})M;\ \forall l \in L \quad (18)$$

$$-\mu_{l,h,t',s'} PL^{max}_l \leq PL^e_{l,h,t',s',s} \leq \mu_{l,h,t',s'} PL^{max}_l;\ \forall l \in L \quad (19)$$

$$0 \leq P^e_{g,h,t',s',s} \leq P^{max}_g \phi_{g,h,t',s'};\ \forall g \in G \quad (20)$$

$$0 \leq PLS^e_{b,h,t',s',s} \leq PD_{b,h,t',s};\ \forall b \in B \quad (21)$$

$$0 \leq PWC^e_{w,h,t',s',s} \leq PW^f_{w,h,t',s} \psi_{w,h,t',s'};\ \forall w \in W \quad (22)$$

The above constraints are similar to the normal operational constraints such that (15) represents the supply-demand power balance constraint at each bus during emergency condition. Constraints (16) and (17) calculate power flow through each new line and enforce their flow limitations, respectively. Similarly, constraint (18) computes the line flow of each existing line, and constraint (19) limits the power flow of each existing line. The binary parameter $\mu_{l,h,t',s'}$ in (18) and (19) is for defining in-service and out-of-service states of lines during emergency condition [22], [23]. In other words, if line l at time interval h, emergency day t', and scenario s' is damaged or connected to a damaged substation (out-of-service state), we set $\mu_{l,h,t',s'} = 0$; otherwise, it is equal to 1. Constraints (20)-(22) represent conventional generator production capacity, load shedding, and wind curtailment constraints, respectively. The binary parameters $\phi_{g,h,t',s'}$ and $\psi_{w,h,t',s'}$ determine if generator g or wind farm w is in-service or out-of-service. If generator g or wind farm w is in a damage state or connected to a damaged substation, we set the associated parameter equal to 0 until the substation is recovered.

C. Damage Scenario Determination

We use a probabilistic approach to obtain the damage scenarios of transmission assets in response to hurricanes. To do so, first, we characterize hurricane events using historical data and HAZUS software [45]. Then, the fragility of components to hurricanes is defined and finally, the algorithm for generating scenarios is presented.

1) Hurricane hazard model: In the case of hurricanes, we need to model their magnitudes, landfall locations and possible trajectories, and spatial wind speed profiles. For the magnitudes, hurricanes are categorized from 1 to 5 based on their maximum wind speeds. The wind speed ranges of each hurricane category with its occurrence probability are provided in [46], [47]. For the locations, we consider a set of probable landfall locations and hurricane trajectories in the study area based on historical hurricane data. Finally, the wind speed profile for each hurricane scenario (landfall location and trajectory) is modeled using a set of circles, as shown in Fig. 2, which their radius is defined based on the worst possible hurricane. In this figure, the wind speed in each area is determined based on wind speed at landfall location and the defined deduction factors using HAZUS software [45], [48]. Accordingly, the area inside the red circle (A1) experience the maximum wind speed while it is dropped to 82.5% of the maximum wind speed for the area between the red circles and the blue circles (A2) [34]. Then, the wind speed decreases to 75% of the values in A1 and A2 for the area inside the orange circle (A3) and between orange and green circles (A4), respectively. The wind speed outside of these areas will not be considered in this paper because the hurricane-induced damage probabilities of assets within these areas are extremely low [45].

2) Components fragility model: We utilize fragility curves to give the probability distribution of damage states as a function of given peak gust speed, which is the highest "instantaneous" wind speed during a specified period (usually 3 seconds) [49], for different network components. These curves for substations, transmission lines, and wind farms are as follows.

Substations: The probability damage functions of substations in response to hurricanes are modeled by log-normal distribution functions (see [39], [48], [50] for detail). Fig. 3 shows the fragility curves for a typical substation. Repair times of substations follow the Normal distribution as $N(72h, 36h)$, $N(168h, 84h)$, and $N(720h, 360h)$ for moderate, severe, and complete damage states, respectively [46], [51].

Transmission lines: Transmission lines consist of a various number of support structures such as towers, conductors, and

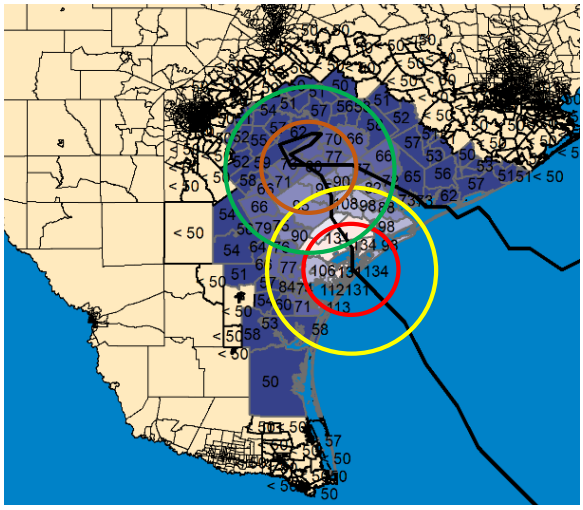

Fig. 2. General wind speed distribution model of hurricanes using HAZUS.

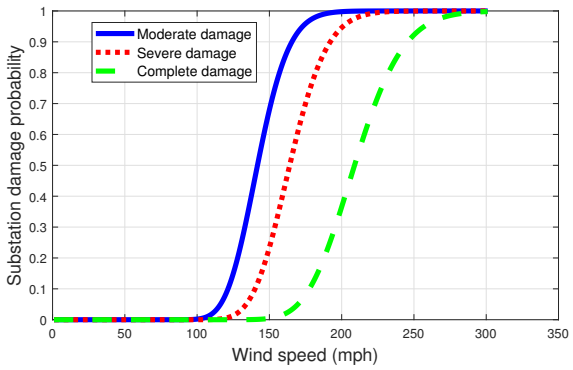

Fig. 3. Fragility curves for a typical substation located in light suburban terrain.

poles. The number of transmission support structures (TSSs) can be calculated by dividing the line length by the average span between two adjacent towers [46]. The failure probability of i^{th} transmission structure can be approximated by an exponential function for a given wind speed ω_g in mph as in (23) [46], [49]. The moderate, severe, and complete damage states for a transmission line are defined as 12%, 50%, and 80% failures of its support structures, respectively [20], [51]. The repair times of a transmission line for moderate, severe, and complete damage states are considered as $N(24h, 12h)$, $N(72h, 36h)$, and $N(168h, 84h)$, respectively [46], [51].

$$pf_{TSS_i}(\omega_g) = min\{2 \times 10^{-7} e^{0.0834\omega_g}, 1\} \tag{23}$$

Wind farms: Wind farms consist of several wind turbines with similar characteristics. The failure probability of a typical wind turbine can be expressed by log-logistic distribution for a given wind speed ω_g as in (24) [52]. In this equation, α and β are scale and shape parameters of the log-logistic distribution, respectively. The values of these parameters are given in [52] for a 5 MW offshore wind turbine designed by the U.S. NREL [53]. Accordingly, the moderate, severe, and complete damage states for a wind farm are defined by 40%, 70%, and 100% failures of wind turbines, respectively [32], [51]. The associated repair times for a wind farm for moderate, severe, and complete damage states are assumed as $N(48h, 24h)$, $N(144h, 72h)$, and $N(336h, 168h)$.

$$pf_{WT}(\omega_g : \alpha, \beta) = \frac{(\omega_g/\alpha)^\beta}{1 + (\omega_g/\alpha)^\beta} \tag{24}$$

3) Scenario generation and reduction: The algorithm to find the damage scenarios of transmission assets in response to hurricane events using the discussed hurricane hazard model and assets' fragility functions is as follows.

- Initialization:
  1) Define a set of possible landfall locations and hurricane paths based on historical data
  2) Determine transmission lines, wind farms, and substations in the areas A1–A4 for each hurricane
- Scenario Generation:
  1) Generate a random number to select one of the hurricane scenarios
  2) Generate a random number for wind speed in A1 based on hurricane category occurrence probability and calculate wind speeds in A2–A4
  3) Calculate the moderate, severe, and complete damage probabilities of each substation using the calculated wind speeds
  4) Calculate the failure probabilities of each TSS and wind turbine using the calculated wind speeds and equations (23) and (24)
  5) Generate a set of random numbers $(u_1, u_2, \ldots, u_k)$ uniformly distributed in $\{0, 1\}$ for each substation, TSS, and wind turbine
  6) Compare $u_1, u_2, \ldots, u_k$ with calculated damage and failure probability values of substations, TSS, and wind turbines
     a) For substations: If u_k is less than complete damage probability, then the asset k is in complete damage condition; else if it is less than severe damage probability, then it is in severe damage condition; else if it is less than moderate damage probability, then it is in moderate damage condition; else it is not damaged
     b) For lines and wind farms: TSS or wind turbine k is failed if the associated u_k is less than the associated failure probability
     c) Determine damage states of each line and wind farm using the failure percentages mentioned above
  7) Generate random numbers to obtain the recovery time of each asset using the repair probability distributions and type of damage
  8) Repeat steps 1 to 7 until the maximum number of scenarios are generated
- Scenario Reduction: Reduce the generated scenarios using available methods such as FFM [40].

III. Solution Procedure

The proposed two-stage stochastic model (1)-(22) can be rewritten in a compact form as:

$$\min_{X,Y^n_{t,s},Y^e_{t',s',s}} C^i X + \sum_{s\in\Omega} p_s \Bigg(\sum_{t\in T} \tau^n_t C^n Y^n_{t,s} + \sum_{s'\in\Omega'} p_{s'} \sum_{t'\in T'} \tau^e_{t',s'} C^e Y^e_{t',s',s} \Bigg) \tag{25}$$

s.t.

$$AX \le B \tag{26}$$

$$D^n X + E^n Y^n_{t,s} = F^n; \forall t, s \ (\lambda_{t,s}) \tag{27}$$

$$G^n X + H^n Y^n_{t,s} \ge I^n; \forall t, s \ (\alpha_{t,s}) \tag{28}$$

$$D^e X + E^e Y^e_{t',s',s} = F^e; \forall t', s', s \ (\gamma_{t',s',s}) \tag{29}$$

$$G^e X + H^e Y^e_{t',s',s} \ge I^e; \forall t', s', s \ (\beta_{t',s',s}) \tag{30}$$

The objective function (25) corresponds to (1)-(4). Constraint (26) represents the investment decision constraints defined as (5) and (6). Constraint (27) and (29) denote the power balance constraints for normal and emergency conditions, i.e., (7) and (15). Constraints (28) and (30) represent the inequality constraints (8)-(14) and (17)-(22) regarding the normal and emergency conditions, respectively. Variable vectors $\lambda_{t,s}$, $\alpha_{t,s}$, $\gamma_{t',s',s}$, and $\beta_{t',s',s}$ are vectors of dual variables associated with the corresponding constraints. Vectors C^i, C^n, and C^e are the investment cost, normal and emergency operation cost vectors, respectively.

The above optimization problem can be recast as a master problem and a set of subproblems based on the dual Benders decomposition framework. The master problem, subproblems, and the solution algorithm are described as follows.

A. Subproblem

The proposed model has two sets of subproblems (SP1, SP2) related to normal and emergency conditions. These subproblems are defined as follows according to the dual Benders decomposition framework [54].

SP1: $\forall s, t$

$$\max_{\lambda_{t,s},\alpha_{t,s}} (F^n - D^n X^*)\lambda_{t,s} + (I^n - G^n X^*)\alpha_{t,s} \tag{31}$$

s.t.

$$E^n \lambda_{t,s} + H^n \alpha_{t,s} = C^n \tag{32}$$

$$\lambda_{t,s} : free \qquad \alpha_{t,s} \ge 0 \tag{33}$$

SP2: $\forall s, s', t'$

$$\max_{\gamma_{t',s',s},\beta_{t',s',s}} (F^e - D^e X^*)\gamma_{t',s',s} + (I^e - G^e X^*)\beta_{t',s',s} \tag{34}$$

s.t.

$$E^e \gamma_{t',s',s} + H^e \beta_{t',s',s} = C^e \tag{35}$$

$$\gamma_{t',s',s} : free \qquad \beta_{t',s',s} \ge 0 \tag{36}$$

The vector X^* is the investment decision which comes from the master problem and considered as input data in the SP1 and SP2.

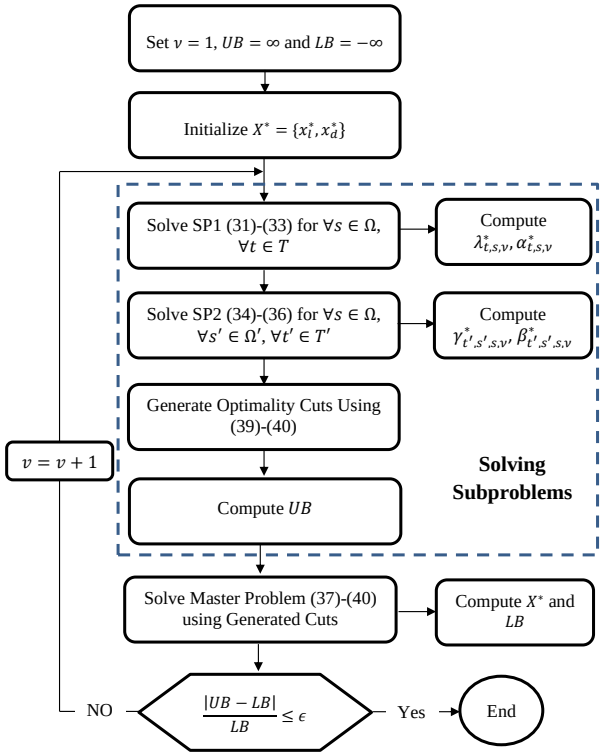

Fig. 4. Flowchart of the solution algorithm.

B. Master Problem

The master problem of the proposed model is as below:

$$\min_X C^i X + \sum_{s\in\Omega} p_s \Big(\sum_{t\in T} \tau^n_t \eta^n_{t,s} + \sum_{s'\in\Omega'} p_{s'} \sum_{t'\in T'} \tau^e_{t',s'} \eta^e_{t',s',s} \Big) \tag{37}$$

s.t.

$$(26) \tag{38}$$

$$\eta^n_{s,t} \ge (F^n - D^n X)\lambda^*_{t,s,v} + (I^n - G^n X)\alpha^*_{t,s,v} \tag{39}$$

$$\eta^e_{t',s',s} \ge (F^e - D^e X)\gamma^*_{t',s',s,v} + (I^e - G^e X)\beta^*_{t',s',s,v} \tag{40}$$

where (39) and (40) are the optimality cuts corresponding to SP1 and SP2, respectively. The v is the iteration counter and vectors $\lambda^*_{t,s,v}$,$\alpha^*_{t,s,v}$, $\gamma^*_{t',s',s,v}$, and $\beta^*_{t',s',s,v}$ are the optimal values of SP1 and SP2 decision variables in iteration v [54]. It should be noted that since we allow wind curtailment and load shedding in the model, the subproblems SP1 and SP2 are always feasible for any given X^*. Therefore, the optimality cuts (39) and (40) are enough and no feasibility check is needed [54].

C. Solution Algorithm

The flowchart of the Benders decomposition method for solving the proposed model is shown in Fig. 4. The steps of the algorithm are described as below [54]:

1) Initialization:
   a) Initialize the lower and upper bounds: $LB = -\infty$ and $UB = \infty$
   b) Initialize feasible values for x^*_l, x^*_d

c) Set the iteration counter $v = 1$

2) Solving subproblems:
   a) Solve SP1 (31)-(33) for each t and s and find $\lambda^*_{t,s,v}$ and $\alpha^*_{t,s,v}$
   b) Solve SP2 (34)-(36) for each t', s', and s and find $\gamma^*_{t',s',s,v}$ and $\beta^*_{t',s',s,v}$
   c) Generate optimality cuts using (39) and (40)
   d) Update upper bound as: $UB = C^i X^* + \sum_{s\in\Omega} p^s \big(\sum_{t\in T} \tau^n_t Z^{n,*}_{t,s} + \sum_{s'\in\Omega'} p^{s'} \sum_{t'\in T'} \tau^e_{t',s'} Z^{e,*}_{t',s',s} \big)$ where $Z^{n,*}_{t,s}$ and $Z^{e,*}_{t',s',s}$ are the objective values of SP1 and SP2, respectively.

3) Solving master problem:
   a) Solve the master problem (37)-(40)
   b) Update lower bound as: $LB = Z^{MP,*}$ where $Z^{MP,*}$ is the objective value of the master problem.

4) Convergence checking:
   a) If $|UB - LB|/LB \leq \epsilon$ stop the algorithm
   b) If not, increment the iteration counter $v = v + 1$ and go to 2.

IV. Simulation Results

The IEEE 118-bus test system [55], which has been mapped to Texas state in [1], is selected for the case study. This system has 186 branches, 54 generator units, and 91 load buses. To modify this system, we add four wind farms with a capacity of 350 MW, 100 MW, 100 MW, and 150 MW in buses 37, 55, 108, and 117, respectively. Besides, the capacity of 500 MVA branches is reduced to 250 MVA while it is set to 120 MVA for other branches to make the network more congested such that the results could show the effectiveness of the model clearer. Note that the seasonal line ratings and the effects of wind-related cooling during storms are not considered in this paper. The detailed data of this test system including the line numbers can be found in [55], [56].

We consider four representative days associated with winter, spring, summer, and fall seasons [57], [58]. Using the historical hourly data from the ERCOT market for the year 2017 [59], we generated one hundred thousand load and wind power scenarios and then reduced them to five scenarios using the FFM [35], [41]. Both penalty factors for load and wind curtailment ($\varkappa^{sh}_b$ and $\varkappa^{wc}_w$) are assumed to be 2000 \$/MWh and the c^{sh}_b is considered to be 1000 \$/MWh for all load buses.

It is assumed that DERs can only be installed in load buses. The size of each DER unit (P^{dg}) is considered 5 MW and maximum of 6 units can be installed in each candidate location. The maximum DER integration is limited to 15% of the peak load, i.e., $\varrho = 0.15$ [35]. The capital cost of each unit is considered to be 1000 \$/kW that is annualized based on its life-time (10 years) and interest rate (2%) [44]. The operational and maintenance cost and the capacity factor of each DER unit are assumed to be 35 \$/MWh and 0.9, respectively [60].

The presented procedure in section II-C is utilized to generate damage scenarios of transmission assets using one of the most probable landfall location and hurricane trajectory in Texas state. The generated damage scenarios are reduced to 5 to be used in the proposed planning model and have tractable results. The final damage scenarios can be found in [56]. It should be mentioned that extreme weather events are assumed to happen in the summer.

TABLE I
Planning Outcomes for the Defined Alternatives.

	TEP-N	DTEP-E	DTEP-N	DTEP-EN
Constructed lines	$l_{8-5}, l_{30-17}, l_{26-30}, l_{12-117}$	$l_{8-5}, l_{30-17}, l_{26-30}, l_{65-68}, l_{83-85}, l_{12-117}$	l_{65-68}, l_{12-117}	l_{83-85}, l_{12-117}
Main nodes of installed DERs	–	$70-107$	$12-67$ & $100-112$	$70-107$
Installed DERs	–	900 MW	900 MW	900 MW
Lines inv. cost	M\$ 1.600	M\$ 2.663	M\$ 0.789	M\$ 0.506
DERs inv. cost	–	M\$ 100	M\$ 100	M\$ 100
Total normal operation cost	M\$ 1847	M\$ 1724	M\$ 1720	M\$ 1725

A. Demonstration of Planning Outcomes for Alternative Cases

In this section, we apply the proposed method to the test case based on the data and damage scenarios mentioned above and discuss the outcomes. We refer to the proposed planning approach, i.e., the joint transmission and DER planning considering both normal and emergency conditions, by DTEP-EN. In addition to the proposed approach, we also demonstrate the planning outcomes for three other alternative approaches, i.e., transmission planning considering only normal condition (TEP-N), joint transmission and DER planning considering only emergency condition (DTEP-E), and joint transmission and DER planning considering only normal condition (DTEP-N).

As expected, different expansion plans are obtained when considering DERs and normal or emergency conditions. Table I summarizes the planning outcomes for the aforementioned alternatives. Observe from the table, four and six new lines are installed for TEP-N (i.e., l_{8-5}, l_{30-17}, l_{26-30}, l_{12-117}) and DTEP-E (i.e., l_{8-5}, l_{30-17}, l_{26-30},l_{65-68}, l_{83-85}, l_{12-117}), respectively, whereas only two new lines are added in DTEP-N (i.e., l_{65-68}, l_{12-117}) and DTEP-EN (i.e., l_{83-85}, l_{12-117})- see the line details in [55], [56]. The line l_{12-117} is common in all four alternatives, whereas one of the lines l_{65-68} or l_{83-85} is chosen for the DTEP-N and DTEP-EN, where only normal or both normal and emergency conditions are considered, respectively. Also, line l_{83-85} is common for DTEP-E and DTEP-EN where the emergency condition is considered. Furthermore, the total installed DER capacity is 900 MW for all three DTEP-N, DTEP-E, and DTEP-EN. The DER units in DTEP-N are mainly installed in buses within the non-impacted area, whereas for DTEP-E and DTEP-EN, they are mostly distributed in the impacted area, as partially shown in Fig. 5. In this figure, the colored nodes indicate the installation of DERs at those nodes; the red and green nodes represent the location of DER units only for DTEP-N or only for DTEP-EN, respectively; the blue nodes indicate the common locations between the two DTEP-N and DTEP-EN alternatives. Also, the DER locations for DTEP-E in this figure are the same as those for DTEP-EN plus node 109 that is not chosen in DTEP-EN. It can be observed from this figure that as expected, considering emergency condition suggests an expansion plan for DER units to support the load in the damaged areas.

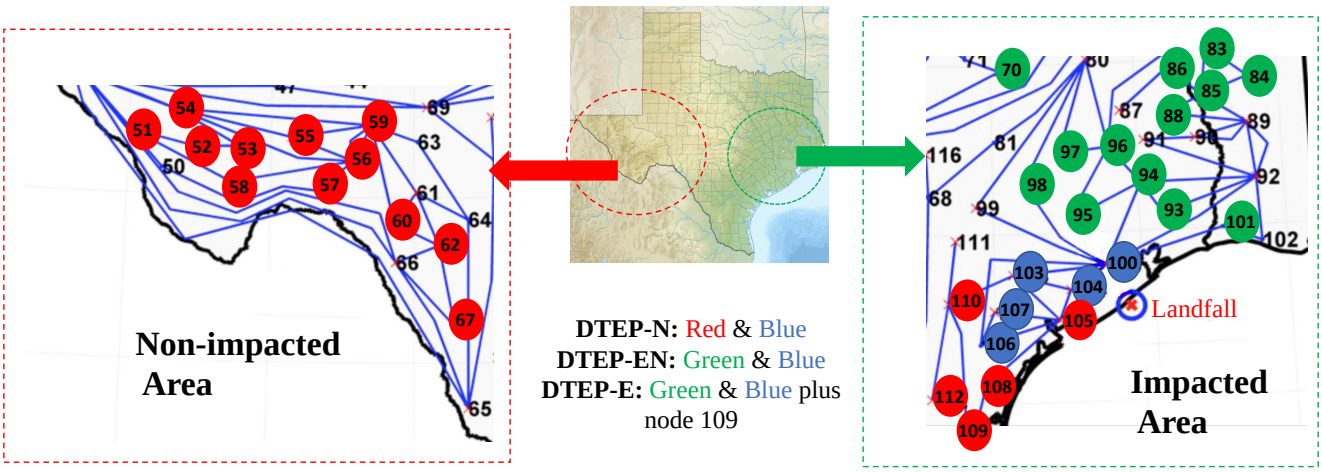

Fig. 5. Installed locations for DER units in impacted and non-impacted regions for the alternatives.

The planning cost, i.e., the sum of the annual operation and investment costs, is very close for the aforementioned alternatives, i.e., B$1.849, B$1.827, B$1.821, and B$1.826 for TEP-N, DTEP-E, DTEP-N, and DTEP-EN, respectively. Note that the investment portion of the total annual cost has gone up when DER is considered. However, since the output power of DERs displaces the expensive peaking generators, the operation cost is lower for DTEP-E, DTEP-N, and DTEP-EN compared with TEP-N. Therefore, the suggested expansion plan in DTEP-EN covers the area where the major event hits under the emergency operation condition, as highlighted in Fig. 5. Also, it helps the system under the normal operating condition similar to DTEP-N by reducing the number of new lines and operation costs. Note that the total investment costs, including the costs of transmission lines and DER units, are almost the same for all three DTEP-E, DTEP-N, and DTEP-EN. However, DTEP-E results in installing four new lines more than DTEP-N and DTEP-EN which can increase the risk of stranded assets.

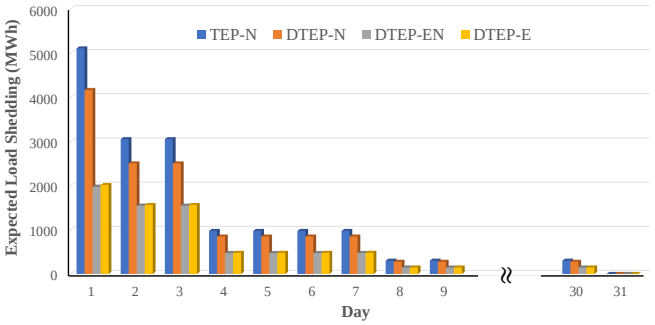

Fig. 6. Expected load shedding of the obtained plans under damage scenarios.

TABLE II
TOTAL EXPECTED LOAD SHEDDING FOR DEFINED ALTERNATIVES.

	Damaged Scenarios (GWh)	Hurricane IKE (GWh)	Hurricane Harvey (GWh)
TEP-N	22.04	10.09	10.03
DTEP-N	18.91	8.95	4.95
DTEP-EN	10.31	4.64	1.99
DTEP-E	10.32	4.71	2.01

B. Resiliency Improvements

This section investigates the resiliency of the test power system for the obtained expansion plans in TEP-N, DTEP-N, DTEP-E, and DTEP-EN under defined damage scenarios and two real-life hurricanes in the state of Texas, i.e., hurricanes IKE 2008 and Harvey 2017. To do this, we use Monte-Carlo simulation (MCS) along with dc optimal power flow (DCOPF) to calculate the expected daily load shedding for the power system reinforced by each expansion alternative. It is worth mentioning that before running the mentioned MCS and DCOPF for the actual hurricanes, the wind speeds of hurricanes in different regions are determined using the HAZUS software [45].

Fig. 6 shows the expected daily load shedding for TEP-N, DTEP-N, DTEP-E, and DTEP-EN alternatives based on the damage scenarios that were used during the planning process. In other words, if the simulated hurricane actually occurs, how the four expanded systems are compared. As can be seen, the expected daily load shedding for DTEP-EN, which is almost the same as that for DTEP-E, is less than those for TEP-N and DTEP-N over the recovery period. In particular, observe that during the first three days after the impact, the load shedding for the proposed plan is significantly lower than the load shedding for the other alternatives.

We also applied the data from hurricanes IKE and Harvey to the alternative plans. Fig. 7a and Fig. 7b show the expected daily load shedding for those plans in response to hurricanes IKE and Harvey, respectively. As expected, the load shedding reduces over time and the first three days experience the most damages to the power system. From Fig. 7, observe that DTEP-EN and DTEP-E plans result in the least expected load shedding for both hurricanes.

Besides, the total expected load shedding for TEP-N, DTEP-N, DTEP-E, and DTEP-EN alternatives are summarized in Table II for defined damage scenarios, hurricane IKE, and hurricane Harvey. Observe from the table, the expected load shedding for DTEP-EN is significantly less than the load shedding for TEP-N and DTEP-N and is very close to the load shedding for DTEP-E. In particular, the proposed plan (DTEP-

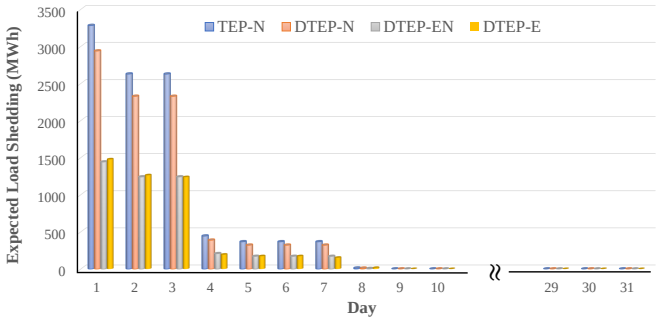

(a) Hurricane IKE

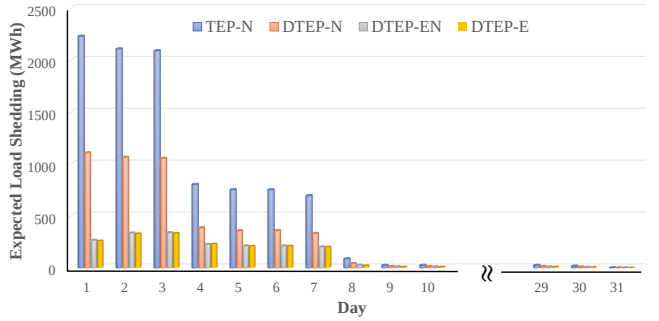

(b) Hurricane Harvey

Fig. 7. Expected load shedding for power network reinforced by TEP-N, DTEP-N, DTEP-E, and DTEP-EN expansion plans against hurricanes Harvey and IKE in Texas state.

EN) leads to 53% and 46% less load shedding under damage scenarios compared to TEP-N and DTEP-N, respectively. Also, the total expected load shedding for this case is 4.64 GWh for hurricanes IKE, i.e., 54% improvement compared with TEP-N and 48% improvement in comparison with DTEP-N. For hurricane Harvey, the total expected load shedding for the case DTEP-EN is 1.99 GWh, i.e., 79% improvement compared with TEP-N and 59% improvement in comparison with DTEP-N. The lower load shedding in the DTEP-EN stems from the installation of the DER units in locations that are more vulnerable to hurricanes.

C. Computational performance

All the simulation cases in this paper have been solved by CPLEX 12.6 under the GAMS environment on a PC running the 64-bit Windows operating system with Core-i7 CPU clocking at 2.2 GHz and 6 GB of RAM. The relative convergence gap for the Benders algorithm has been set to 0.05%. Table III shows the number of discrete variables of the master problem as well as the number of normal and emergency subproblems at each iteration. In the table, parameters n_T, n_S, $n_{T'}$, and n'_S are the number of representative days and scenarios in normal and emergency conditions, respectively. Also, n_{L^+} and n_D are the number of candidate lines and DER locations, respectively. The average computation time of TEP-N, DTEP-N, DTEP-E, and DTEP-EN for the presented case study which includes $n_{L^+} = 17$, $n_D = 91$, $n_T = 4$, $n_S = 5$, $n_{T'} = 3$, and $n'_S = 5$ are 52 min, 18 min, 482 min, and 49 min, respectively. Also, the number of iterations for TEP-N, DTEP-N, DTEP-E, and DTEP-EN are 90, 42, 100, and 20, respectively, in which

TABLE III
COMPUTATIONAL PERFORMANCE OF PLANNING ALTERNATIVE.

	# of Discrete Variables	# of SP1 per iteration	# of SP2 per iteration
TEP-N	n_{L^+}	$n_T \times n_S$	–
DTEP-N	$n_D + n_{L^+}$	$n_T \times n_S$	–
DTEP-E	$n_D + n_{L^+}$	–	$n_{T'} \times n_{S'} \times n_S$
DTEP-EN	$n_D + n_{L^+}$	$n_T \times n_S$	$n_{T'} \times n_{S'} \times n_S$

20 subproblems are solved at each iteration for both TEP-N and DTEP-N whereas DTEP-E and DTEP-EN need to solve 75 and 95 subproblems per iteration, respectively. Note that although the number of subproblems that must be solved in each iteration for DTEP-EN is more than that of other cases, the Benders algorithm has been converged faster due to a bigger number of generated cuts at each iteration. Therefore, the inclusion of both normal and emergency conditions does not necessarily increase the computation time significantly. Moreover, since most of the computation time is spent on solving the subproblems, they can be solved in parallel to improve computation time.

V. CONCLUSION

In this paper, a new planning formulation was proposed to model the expansion of the transmission system and distributed energy resources (DERs) considering power system resiliency. In the model, both normal and emergency conditions and the duration of each condition were considered. The moderate, severe, and complete damage states of lines, substations, and wind farms were considered in emergency scenarios and their recovery times were modeled in the formulation. The obtained formulation was applied to the IEEE 118-bus test system mapped to the state of Texas and was solved using the Benders decomposition approach. Using the wind data of hurricanes IKE and Harvey in Texas state, the response of the proposed system expansion was measured in terms of total expected load shedding over a 31-day period. The proposed plan was compared to three system expansion alternatives, i.e., only considering transmission lines (TEP-N), considering transmission lines and DER units but only accounting for normal operation condition (DTEP-N), and considering transmission lines and DER units for only emergency operation condition (DTEP-E).

The simulation results show that the proposed planning method leads to significantly lower load shedding, particularly during the first three days after the impact. This is owed to the placement of DER units in more vulnerable spots in the system. As expected, the investment cost in the proposed plan is higher than that of TEP-N. However, the total operation and investment costs for the two are very close. This is because the DER units displace some expensive peaking units during normal operations. Furthermore, compared to DTEP-N, the investment and operation costs are very similar; however, the proposed method results in significantly higher resiliency for the system. Moreover, although the resiliency of the proposed plan and DTEP-E are very similar, DTEP-E leads to more number of new lines and results in an over-design plan.

Future work will focus on the extension of the proposed joint transmission and DER planning model to incorporate

weather-related cascading outages. Moreover, transmission switching (TS) was not considered in this study. TS creates new challenges in the operation of the power system under the emergency conditions such as voltage security and dynamic stability which needs to be taken into account. Also, considering TS in the model, makes the subproblems non-convex due to the addition of binary variables. Thus, a new decomposition method will be incorporated to solve the optimization problem. Moreover, the current model is a static planning model that does not consider the impact of climate change and load growth during the planning years. Therefore, the model will be extended as a dynamic planning formulation to consider long-term planning factors. Besides, the work may be extended by including a detailed model for hurricane-induced damages of power system components to consider the effects of flooding and flying debris.

REFERENCES

[1] P. Javanbakht and S. Mohagheghi, "A risk-averse security-constrained optimal power flow for a power grid subject to hurricanes," *Electric Power Systems Research*, vol. 116, pp. 408–418, 2014.

[2] P. Hines, J. Apt, and S. Talukdar, "Large blackouts in north america: Historical trends and policy implications," *Energy Policy*, vol. 37, no. 12, pp. 5249–5259, 2009.

[3] Executive Office of the President, "Economic benefit of increasing electric grid resilience to weather outages," U.S. Department of Energy's Office of Electricity Delivery and Energy Reliability, Tech. Rep., 2013.

[4] Office of Electricity Delivery and Energy Reliability, "Comparing the impacts of northeast hurricanes on energy infrastructure," U.S. Department of Energy, Tech. Rep., 2013.

[5] M. Panteli, D. N. Trakas, P. Mancarella, and N. D. Hatziargyriou, "Boosting the power grid resilience to extreme weather events using defensive islanding," *IEEE Transactions on Smart Grid*, vol. 7, no. 6, pp. 2913–2922, 2016.

[6] W. Li, *Risk assessment of power systems: models, methods, and applications*. John Wiley & Sons, 2014.

[7] North American Electric Reliability Corporation (NERC), "Reliability coordinator operational analyses and real-time assessments," NERC standard, IRO-008-1, Tech. Rep., 2014.

[8] E. Ciapessoni, D. Cirio, A. Pitto, M. Van Harte, M. Panteli, and C. Mak, "Defining power system resilience," *Electra CIGRE J*, vol. 306, pp. 32–34, 2019.

[9] M. Chaudry, P. Ekins, K. Ramachandran, A. Shakoor, J. Skea, G. Strbac, X. Wang, and J. Whitaker, "Building a resilient uk energy system," 2011.

[10] C. O'Hara, "Grid resilience in regional transmission organizations and independent system operators," PJM Document No. AD18-7-000, Tech. Rep., 2018.

[11] M. Panteli and P. Mancarella, "Modeling and evaluating the resilience of critical electrical power infrastructure to extreme weather events," *IEEE Systems Journal*, vol. 11, no. 3, pp. 1733–1742, 2015.

[12] M. Amirioun, F. Aminifar, H. Lesani, and M. Shahidehpour, "Metrics and quantitative framework for assessing microgrid resilience against windstorms," *International Journal of Electrical Power & Energy Systems*, vol. 104, pp. 716–723, 2019.

[13] Z. Li, M. Shahidehpour, F. Aminifar, A. Alabdulwahab, and Y. Al-Turki, "Networked microgrids for enhancing the power system resilience," *Proceedings of the IEEE*, vol. 105, no. 7, pp. 1289–1310, 2017.

[14] M. Panteli and P. Mancarella, "Influence of extreme weather and climate change on the resilience of power systems: Impacts and possible mitigation strategies," *Electric Power Systems Research*, vol. 127, pp. 259–270, 2015.

[15] A. Gholami, T. Shekari, F. Aminifar, and M. Shahidehpour, "Microgrid scheduling with uncertainty: The quest for resilience," *IEEE Transactions on Smart Grid*, vol. 7, no. 6, pp. 2849–2858, 2016.

[16] M. H. Amirioun, F. Aminifar, and M. Shahidehpour, "Resilience-promoting proactive scheduling against hurricanes in multiple energy carrier microgrids," *IEEE Transactions on Power Systems*, 2018.

[17] H. Gao, Y. Chen, Y. Xu, and C.-C. Liu, "Resilience-oriented critical load restoration using microgrids in distribution systems," *IEEE Transactions on Smart Grid*, vol. 7, no. 6, pp. 2837–2848, 2016.

[18] A. Gholami, T. Shekari, and S. Grijalva, "Proactive management of microgrids for resiliency enhancement: An adaptive robust approach," *IEEE Transactions on Sustainable Energy*, 2017.

[19] T. Ding, Y. Lin, Z. Bie, and C. Chen, "A resilient microgrid formation strategy for load restoration considering master-slave distributed generators and topology reconfiguration," *Applied energy*, vol. 199, pp. 205–216, 2017.

[20] N. R. Romero, L. K. Nozick, I. D. Dobson, N. Xu, and D. A. Jones, "Transmission and generation expansion to mitigate seismic risk," *IEEE Transactions on Power Systems*, vol. 28, no. 4, pp. 3692–3701, 2013.

[21] J. Qiu, H. Yang, Z. Y. Dong, J. Zhao, F. Luo, M. Lai, and K. P. Wong, "A probabilistic transmission planning framework for reducing network vulnerability to extreme events," *IEEE Transactions on Power Systems*, vol. 31, no. 5, pp. 3829–3839, 2015.

[22] J. Yan, B. Hu, K. Xie, J. Tang, and H.-M. Tai, "Data-driven transmission defense planning against extreme weather events," *IEEE Transactions on Smart Grid*, vol. 11, no. 3, pp. 2257–2270, 2019.

[23] Y.-P. Fang, C. Fang, E. Zio, and M. Xie, "Resilient critical infrastructure planning under disruptions considering recovery scheduling," *IEEE Transactions on Engineering Management*, 2019.

[24] X. Liu, K. Hou, H. Jia, J. Zhao, L. Mili, X. Jin, and D. Wang, "A planning-oriented resilience assessment framework for transmission systems under typhoon disasters," *IEEE Transactions on Smart Grid*, 2020.

[25] M. Shivaie, M. Kiani-Moghaddam, and P. D. Weinsier, "Resilience-based tri-level framework for simultaneous transmission and substation expansion planning considering extreme weather-related events," *IET Generation, Transmission & Distribution*, vol. 14, no. 16, pp. 3310–3321, 2020.

[26] ——, "A vulnerability-constrained quad-level model for coordination of generation and transmission expansion planning under seismic-and terrorist-induced events," *International Journal of Electrical Power & Energy Systems*, vol. 120, p. 105958, 2020.

[27] A. Soroudi, P. Maghouli, and A. Keane, "Resiliency oriented integration of DSRs in transmission networks," *IET Generation, Transmission & Distribution*, vol. 11, no. 8, pp. 2013–2022, 2017.

[28] W. Yuan, J. Wang, F. Qiu, C. Chen, C. Kang, and B. Zeng, "Robust optimization-based resilient distribution network planning against natural disasters," *IEEE Transactions on Smart Grid*, vol. 7, no. 6, pp. 2817–2826, 2016.

[29] R. Eskandarpour, H. Lotfi, and A. Khodaei, "Optimal microgrid placement for enhancing power system resilience in response to weather events," in *2016 North American Power Symposium (NAPS)*. IEEE, 2016, pp. 1–6.

[30] P. Cicilio, L. Swartz, B. Vaagensmith, C. Rieger, J. Gentle, T. McJunkin, and E. Cotilla-Sanchez, "Electrical grid resilience framework with uncertainty," *Electric Power Systems Research*, vol. 189, p. 106801, 2020.

[31] B. Zhang, P. Dehghanian, and M. Kezunovic, "Optimal allocation of pv generation and battery storage for enhanced resilience," *IEEE Transactions on Smart Grid*, vol. 10, no. 1, pp. 535–545, 2017.

[32] T. Lagos, R. Moreno, A. N. Espinosa, M. Panteli, R. Sacaan, F. Ordonez, H. Rudnick, and P. Mancarella, "Identifying optimal portfolios of resilient network investments against natural hazards, with applications to earthquakes," *IEEE Transactions on Power Systems*, vol. 35, no. 2, pp. 1411–1421, 2019.

[33] E. A. Paaso, J. E. Svachula, and S. Bahramirad, "Planning and operations of the utility of the future in illinois," *The Electricity Journal*, vol. 28, no. 10, pp. 18–28, 2015.

[34] S. Ma, B. Chen, and Z. Wang, "Resilience enhancement strategy for distribution systems under extreme weather events," *IEEE Transactions on Smart Grid*, vol. 9, no. 2, pp. 1442–1451, 2016.

[35] H. Ranjbar and S. H. Hosseini, "Stochastic multi-stage model for co-planning of transmission system and merchant distributed energy resources," *IET Generation, Transmission & Distribution*, 2019.

[36] H. Ranjbar, S. H. Hosseini, and H. Zareipour, "A robust optimization method for co-planning of transmission systems and merchant distributed energy resources," *International Journal of Electrical Power & Energy Systems*, vol. 118, p. 105845, 2020.

[37] Z. Parvini, A. Abbaspour, M. Fotuhi-Firuzabad, and M. Moeini-Aghtaie, "Operational reliability studies of power systems in the presence of energy storage systems," *IEEE Transactions on Power Systems*, vol. 33, no. 4, pp. 3691–3700, 2017.

[38] V. Hinojosa and J. Velásquez, "Stochastic security-constrained generation expansion planning based on linear distribution factors," *Electric Power Systems Research*, vol. 140, pp. 139–146, 2016.

[39] J. Winkler, L. Duenas-Osorio, R. Stein, and D. Subramanian, "Performance assessment of topologically diverse power systems subjected to hurricane events," *Reliability Engineering & System Safety*, vol. 95, no. 4, pp. 323–336, 2010.

[40] H. Heitsch and W. Römisch, "Scenario reduction algorithms in stochastic programming," *Computational optimization and applications*, vol. 24, no. 2-3, pp. 187–206, 2003.

[41] S. Pineda and A. Conejo, "Scenario reduction for risk-averse electricity trading," *IET generation, transmission & distribution*, vol. 4, no. 6, pp. 694–705, 2010.

[42] H. Park and R. Baldick, "Transmission planning under uncertainties of wind and load: Sequential approximation approach," *IEEE Transactions on Power Systems*, vol. 28, no. 3, pp. 2395–2402, 2013.

[43] H. Shayeghi and A. Bagheri, "Dynamic sub-transmission system expansion planning incorporating distributed generation using hybrid dcga and lp technique," *International Journal of Electrical Power & Energy Systems*, vol. 48, pp. 111–122, 2013.

[44] S. Dehghan and N. Amjady, "Robust transmission and energy storage expansion planning in wind farm-integrated power systems considering transmission switching," *IEEE Transactions on Sustainable Energy*, vol. 7, no. 2, pp. 765–774, 2015.

[45] Federal Emergency Management Agency, "Hazus multi-hazard." [Online]. Available: https://www.fema.gov/hazus-software

[46] M. Ouyang and L. Duenas-Osorio, "Multi-dimensional hurricane resilience assessment of electric power systems," *Structural Safety*, vol. 48, pp. 15–24, 2014.

[47] National oceanic and atmospheric administration (NOAA), "Hurricane basics," U.S. Department of commerce, Tech. Rep., 1999.

[48] H. Ranjbar, S. H. Hosseini, and H. Zareipour, "Hurricane induced damage scenario determination of transmission network components," presented at the 2020 IEEE PES general meeting, August 2020.

[49] R. Brown, "Cost-benefit analysis of the deployment of utility infrastructure upgrades and storm hardening programs," *Quanta Technology, Raleigh*, 2009.

[50] A. F. Mensah, "Resilience assessment of electric grids and distributed wind generation under hurricane hazards," Ph.D. dissertation, 2015.

[51] "Hazus-mh4 multi-hazard loss estimation methodology, earthquake model-technical manual," Federal Emergency Management Agency (FEMA), Tech. Rep., 2003. [Online]. Available: https://www.fema.gov/media-library-data/20130726-1820-25045-6286/hzmh2_1_eq_tm.pdf

[52] S. Rose, P. Jaramillo, M. J. Small, and J. Apt, "Quantifying the hurricane catastrophe risk to offshore wind power," *Risk analysis*, vol. 33, no. 12, pp. 2126–2141, 2013.

[53] J. Jonkman, S. Butterfield, W. Musial, and G. Scott, "Definition of a 5-mw reference wind turbine for offshore system development," National Renewable Energy Lab.(NREL), Golden, CO (United States), Tech. Rep., 2009.

[54] A. J. Conejo, E. Castillo, R. Minguez, and R. Garcia-Bertrand, *Decomposition techniques in mathematical programming: engineering and science applications*. Springer Science & Business Media, 2006.

[55] "IEEE 118-bus system data," Electrical and Computer Engineering Department, Illinois Institute of Technology (IIT), Tech. Rep. [Online]. Available: http://motor.ece.iit.edu/Data/JEAS_IEEE118.doc

[56] "The detail data of utilized ieee 118-bus test case." [Online]. Available: https://onedrive.live.com/redir?resid=CC0057D012D7B730%2121025&authkey=%21AOCQg6ppKVv9eHA&page=Download

[57] H. Saber, M. Moeini-Aghtaie, M. Ehsan, and M. Fotuhi-Firuzabad, "A scenario-based planning framework for energy storage systems with the main goal of mitigating wind curtailment issue," *International Journal of Electrical Power & Energy Systems*, vol. 104, pp. 414–422, 2019.

[58] C. Grigg, P. Wong, P. Albrecht, R. Allan, M. Bhavaraju, R. Billinton, Q. Chen, C. Fong, S. Haddad, S. Kuruganty *et al.*, "The ieee reliability test system-1996. a report prepared by the reliability test system task force of the application of probability methods subcommittee," *IEEE Transactions on power systems*, vol. 14, no. 3, pp. 1010–1020, 1999.

[59] "Wind power production - hourly averaged actual and forecasted values by geographical region," 2017. [Online]. Available: http://www.ercot.com/gridinfo/generation.

[60] L. Goldstein, B. Hedman, D. Knowles, S. I. Freedman, R. Woods, and T. Schweizer, "Gas-fired distributed energy resource technology characterizations," National Renewable Energy Lab., Golden, CO.(US), Tech. Rep., 2003.

Hossein Ranjbar received the M.Sc. and Ph.D. degrees in electrical engineering from the Sharif University of Technology, Tehran, Iran, in 2014 and 2021, respectively.

From November 2018 to July 2020, he was a Visiting Researcher with the Department of Electrical and Computer Engineering, University of Calgary, Calgary, AB, Canada. His fields of interest include power system planning and operation, renewable energy integration, as well as optimization and its application in power systems.

Seyed Hamid Hosseini (Member, IEEE) received the Ph.D. degree in electrical engineering from the Iowa State University, Ames, IA, USA, in 1988.

Since 1988, he has been with the Department of Electrical Engineering, Sharif University of Technology, Tehran, Iran, where currently he is a Full Professor. His current research interests include power system operation, optimization, planning, and renewable energy

Hamidreza Zareipour (Senior Member, IEEE) received the Ph.D. degree in electrical engineering from University of Waterloo, Waterloo, ON, Canada, in 2006. He is currently a Professor with the Department of Electrical and Computer Engineering, University of Calgary, Calgary, AB, Canada. His research focuses on economics, planning, and management of power and energy systems in a deregulated electricity market environment.